



HAL
open science

Electrochemical fabrication of oriented ZnO nanorods on TiO₂ nanotubes

G. Jimenez Cadena, Marielle Eyraud, C. Chassigneux, Florence Vacandio, E. Comini, G. Sberveglieri, T. Djenizian

► **To cite this version:**

G. Jimenez Cadena, Marielle Eyraud, C. Chassigneux, Florence Vacandio, E. Comini, et al.. Electrochemical fabrication of oriented ZnO nanorods on TiO₂ nanotubes. *Int. J. Nanotechnol.*, 2012, 9 (3/4/5/6/7), pp.3 - 7. 10.1504/IJNT.2012.045333 . hal-02656763

HAL Id: hal-02656763

<https://amu.hal.science/hal-02656763>

Submitted on 5 Jun 2020

HAL is a multi-disciplinary open access archive for the deposit and dissemination of scientific research documents, whether they are published or not. The documents may come from teaching and research institutions in France or abroad, or from public or private research centers.

L'archive ouverte pluridisciplinaire **HAL**, est destinée au dépôt et à la diffusion de documents scientifiques de niveau recherche, publiés ou non, émanant des établissements d'enseignement et de recherche français ou étrangers, des laboratoires publics ou privés.



Distributed under a Creative Commons Attribution - NoDerivatives 4.0 International License

Electrochemical fabrication of oriented ZnO nanorods on TiO₂ nanotubes

Marielle Eyraud*

Aix-Marseille Univ CNRS,
Laboratoire Chimie Provence,
Electrochemistry of Materials Research Group, Centre Saint Jerome 13397 Marseille Cedex 20, France
E-mail: marielle.eyraud@univ-provence.fr

G. Jimenez-Cadena

INFM-CNR SENSOR,
Lab and University of Brescia, Via Valotti 9, 25133 Brescia, Italy E-mail: giselle.jimenez@ing.unibs.it

C. Chassigneux and F. Vacandio

Aix-Marseille Univ CNRS,
Laboratoire Chimie Provence,
Electrochemistry of Materials Research Group, Centre Saint Jerome 13397 Marseille Cedex 20, France
E-mail: carine.chassigneux@univ-provence.fr E-mail: Florence.vacandio@univ-provence.fr

E. Comini and G. Sberveglieri

SENSOR,
University of Brescia and CNR-IDASC, Via Valotti 9, 25133 Brescia, Italy
E-mail: comini@ing.unibs.it E-mail: giorgio.sberveglieri@ing.unibs.it

T. Djenizian

Aix-Marseille Univ CNRS,
Laboratoire Chimie Provence,
Electrochemistry of Materials Research Group, Centre Saint Jerome 13397 Marseille Cedex 20, France E-mail: thierry.djenizian@univ-provence.fr

Abstract: We report the ability to use TiO₂ nanotube as a guide layer to achieve the vertical growth of ZnO nanorods, in additive-free bath. First, we focused on the anodisation conditions (cell voltage and anodisation time) to produce TiO₂ nanotube thin films grown from a 1.5 μm thick Ti layer sputtered onto Si. Highly organised titania nanotubes were obtained in glycerol viscous electrolyte. In a second step, the electrochemical growth of ZnO grains has been investigated from a zinc nitrate bath at 70°C on both Ti foil and TiO₂ nanotubes. ZnO deposition mechanism has been highlighted through the electrochemical experiments in conjunction with XRD technique and scanning electron microscopy (SEM) examinations. On Ti foils, we show that addition of additives is required to obtain a highly oriented nanostructured ZnO deposit. On TiO₂ nanotubes, additives are not necessary to obtain such a deposit: Titania nanotubes can be used to guide the vertical growth of hybrid nano-architected ZnO/TiO₂ electrode.

Keywords: zinc oxide; titania nanotubes; composite nano-architected electrode; electrochemical methods.

1 Introduction

During the last decades, titanium dioxide (TiO₂) has become a very promising material because of multiple applications [1,2]. Particularly, the different structures of TiO₂ have been successfully used for photocatalysis, gas sensing, Li batteries, electronic devices and solar cells [1,3–9]. Although TiO₂ nanoparticles have been used for several applications, the electronic transportation phenomenon limits the efficiency of the material owing to the grain boundaries in the semiconductor. Recently, the use of one-dimensional nanostructures like nanowires and nanotubes has shown a significant improvement of the electronic transport. Moreover, nanotubes offer the option of heterogeneous materials [10,11] opening new perspectives for the development of devices based on photocatalysis and photochemical properties.

With several advantages such as high reproducibility, low temperature operation and the ability to control accurately the size structures on various substrates [12–16], the electrochemical approach is highly appreciated to fabricate 1D nanostructures. The first methods to grow nanostructured TiO₂ and self-organised TiO₂ nanotubes were based on simple anodisation procedures performed in acidic electrolytes containing fluoride ions [17,18]. The nanotubes are formed as a result of a competition between the electrochemical growth and the selective chemical dissolution of the oxide layer [19]. Further progress was recently achieved on bulk Ti foils by using viscous electrolyte containing fluoride ions for which smoother tubes can be grown compared with viscous electrolyte [20]. Very few works about electrochemical oxidation of Ti thin film in viscous electrolyte can be found [21].

Because of several remarkable properties [22–24], ZnO is a II-VI semiconductor material widely used for many applications and particularly for the fabrication of photovoltaic devices. ZnO can be synthesised not only using template-based processing [25,26], hydrothermal method [27], wet technique [28] and metal organic chemical vapour deposition [29] but also by electrodeposition process. The one-step electrodeposition of ZnO films was first reported by Izaki and Omi [30] using nitrate ions as oxygen precursor. More results have been reported by Pauporte and Lincot [31], Peulon and Lincot [32] and Ramirez et al. [33] using dissolved oxygen at 70°C. The synthesis of ZnO nanowires has also been achieved by a template technique [26,34]. This method consists of filling the pores of a nanoporous insulating membrane (typically anodic alumina or polycarbonate membranes) that can be subsequently removed after the electrodeposition process. Template-free strategies reported also the use of different additives to tailor the size and morphology of the electrodeposited ZnO crystallites [35]. Among them, hexamethylenetetramine (HMT) seems to produce highly oriented ZnO rods. In a recent work of Welling et al. [36], the influence of deposition potential on the crystallographic structure and transparency of ZnO film deposited on ITO has also been reported.

Both TiO₂ nanotubes and ZnO nanowires have been proposed separately for the fabrication of dye-sensitised solar cell (DSSC) [37,38] and photoelectrocatalytic applications. It has also been shown that the combination of TiO₂ and ZnO can improve the efficiency of solar cell [27,39] or photoelectrocatalytic activity [40]. In these papers, TiO₂ films were obtained either as slurry spread on glass [27] or by anodisation in acid solutions containing fluoride ions [39,40], whereas ZnO layers were deposited using a hydrothermal method with zinc nitrate solution containing HMT at 92°C for 24 h [27] or by successive ionic adsorption and reaction method [39] or cathodic deposition [40]. However, the development of low-cost and weak energy consuming approaches has still to be considered to achieve the fabrication of such a tandem material.

In this paper, the fabrication of TiO₂-ZnO hybrid nanomaterials is achieved by simply using a two-step electrochemical technique. Titania nanotubes were obtained from the anodisation of Ti thin film in a glycerol-containing electrolyte. The effects of applied potential and anodisation time upon the morphology of TiO₂ nanotubes have been analysed. Then, the electrochemical growth of ZnO rods on Ti foils and on TiO₂ nanotubes has been studied. In agreement with previous works recently reported in the case of tin nanowire [41–45], we show that the titania nanotubes could be used as a guide layer to activate the electrochemical growth of vertical ZnO nanomaterials.

2 Experimental

2.1 Titanium thin film on Si

First, Ti thin films were deposited on *p*-type Si (100) substrates with a resistivity of 1–10 Ω cm (Wafer World, Inc.). Before sputtering, Si samples were sonicated for 20 min alternatively in acetone, isopropanol and methanol, rinsed with deionised water and dried under argon stream. To remove the native oxide layer, the Si substrates were dipped in 1% HF solution during 30 s, then rinsed in deionised water, and dried under argon stream. Ti (99.99% purity) was the sputtering target and the base chamber pressure prior to deposition was kept below 10⁻⁷ Torr. The Si substrates were not heated during

the procedure. The high purely argon pressure and the target current during deposition were 6×10^{-4} Torr and 150 mA, respectively. Under these conditions, the deposition rate was 12.5 nm/min. In this work, Ti layer of approximately 1.5 μm thick with a columnar morphology was obtained after two hours.

2.2 *Titania nanotubes*

Titania nanotubes were obtained from the anodisation of the Ti thin films at room temperature ($\sim 25^\circ\text{C}$) using a two-electrode configuration (Ti thin film as working electrode and a Pt grid as counter electrode). Glycerol (GPR Rectapur 24387.292) +1.3% NH₄F (98% Aldrich 12125-01-8) +2% water served as viscous electrolyte. Different potentials were applied during 10 min using a potentiostat Parstat 2273 (EGG). The influence of the anodisation time at a constant applied potential on the growth of titania nanotubes was also checked. After anodisation, the samples were rinsed with deionised water and dried in argon stream.

2.3 *Zinc oxide deposition*

Zinc oxide deposition was first studied using voltammetric experiments in a three-electrode configuration. The equipment consisted in an EGG-PAR model 273 potentiostat-galvanostat. The working electrodes studied were Ti foil. A Pt grid was used as counter electrode and Ag-AgCl KCl saturated as reference electrode. The experiments were done at 70°C in an aqueous solution of Zn(NO₃)₂ (98% 10196-18-6 Sigma-Aldrich) 0.005 M with or without additive: HMT (C₆H₁₂N₄ 99% 100-97-0 Aldrich) 0.005 M. The pH of the as-prepared solution was almost 5. From voltammetric study, some reduction potentials were chosen to obtain bulk ZnO deposits. The same procedure was carried out on TiO₂ nanotube layers to fabricate ZnO/TiO₂ hybrid nanomaterial.

2.4 *Characterisations*

Atomic Force Microscopy (AFM) measurements in contact mode (CP auto probe provided by Park Scientific Instrument) were performed on Ti thin film and Ti foil to assess the roughness of the surface. SEM images (Philips XL-30 FEG) were used to study the morphology of the titania nanotubes and ZnO deposits. XRD experiments (D5000 diffractometer, with Cu K α radiation) were performed to analyse the ZnO layer electrochemically grown directly onto Ti foil and titania nanotubes.

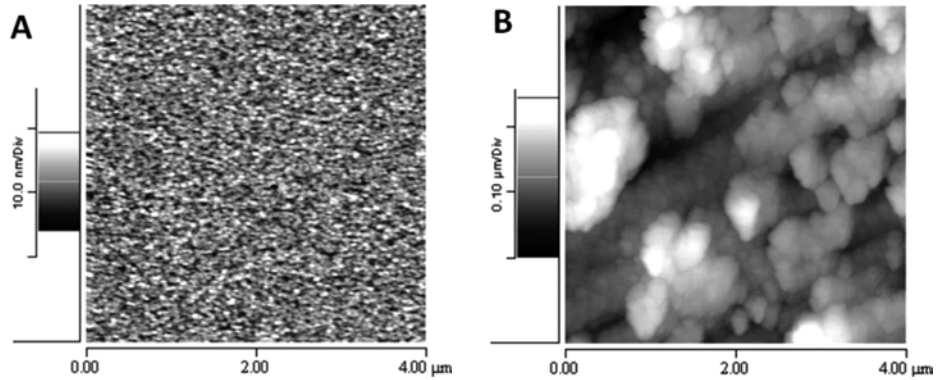
3 **Results and discussion**

3.1 *Titania nanotubes*

The roughness of the Ti layer has a strong influence on the morphology of the titania nanotubes. A decrease in roughness improves the quality of the nanotube arrays. The AFM image of sputtered Ti thin film before anodisation is shown in Figure 1(A). The deposit is homogeneous with a very low roughness (Rms = 2.6 nm) and an average size of Ti grains of around 60 nm. Compared with Ti foil substrate (Figure 1(B)), it is

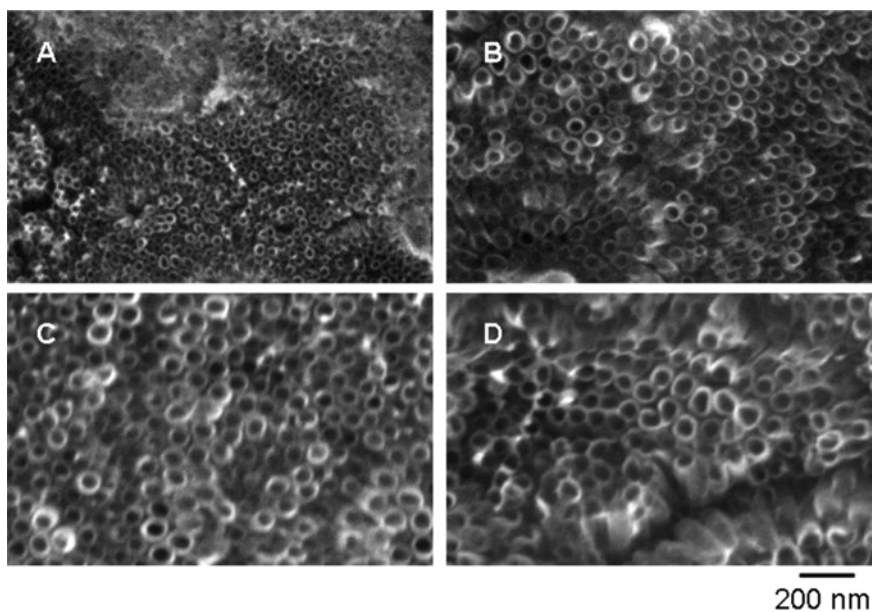
clearly apparent that the roughness is higher ($R_{ms} = 41 \text{ nm}$) and the Ti grain size is significantly larger (approximately 160 nm).

Figure 1 AFM images of (A) sputtered Ti thin film on Si and (B) Ti foil



To understand the influence of the applied potential on the morphology of the nanotubes, Ti thin films were anodised during 10 min in glycerol-containing electrolyte for potential ranging from 40 V to 90 V. From SEM images shown in Figure 2, the diameter of the nanotubes increases with increasing voltage. For an applied potential of 40, 60, 80 and 90 V, the corresponding diameter is around 35, 40, 60–90 and 60–90 nm, respectively. Then, the diameter is more homogeneous at low potential. It can be noted that the layer reveals the presence of cracks when the applied voltage is higher (Figure 2(D)) weakening the mechanical properties of the film. Then, the anodisation voltage has been assessed at 60 V.

Figure 2 SEM images of Ti thin film anodised during 10 min in glycerol-containing electrolyte at applied potential of 40V (A) 60V (B), 80 V (C) and 90V (D)



Cross-sectional SEM images were taken for several anodisation times (Figure 3). The rate of TiO_2 growth and Ti layer consumption was analysed for 0, 10, 20 and 40 min. From Figure 3(A), the initial Ti layer presents a columnar structure with an initial thickness of $1.5\ \mu\text{m}$, which is consistent with previous work [46]. Figure 3(B)–(D) depicts the cross-sectional views of anodised samples carrying vertical arrays of self-organised TiO_2 nanotubes. In agreement with the literature [20], the tubes grown in glycerol-containing electrolyte are smoother with more homogeneous morphological properties than those obtained in very similar conditions by our group in aqueous electrolyte [46]. For anodisation time below 10 min, the rate of TiO_2 growth is approximately $150\ \text{nm}/\text{min}$. Then, the titania growth rate is found to be $40\text{--}50\ \text{nm}/\text{min}$ after 10 min of anodisation. The rate of Ti consumption was about $40\ \text{nm}/\text{min}$ and shows also a decrease until $10\ \text{nm}/\text{min}$. The dependence of the thickness vs. time (Figure 4) suggests a first-order reaction dependent on the Ti concentration.

Figure 3 Cross-sectional SEM images of Ti thin films before anodisation in glycerol-containing electrolyte (A) and after potentiostatic experiments by applying a potential of 60 V during 10 min (B), 20 min (C) and 40 min (D)

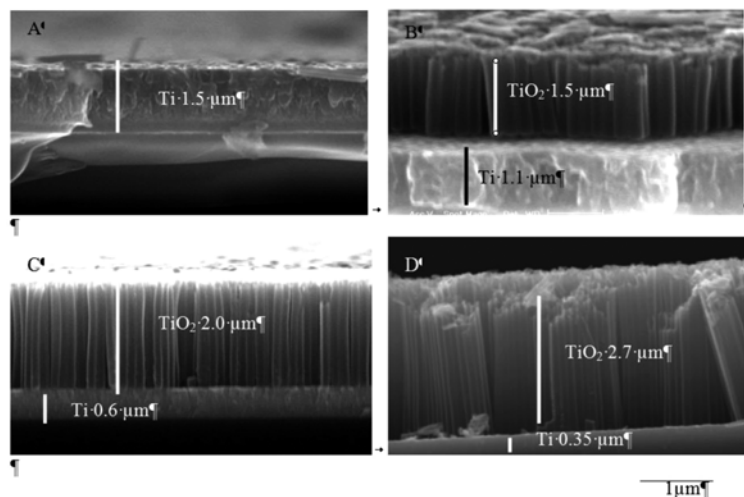
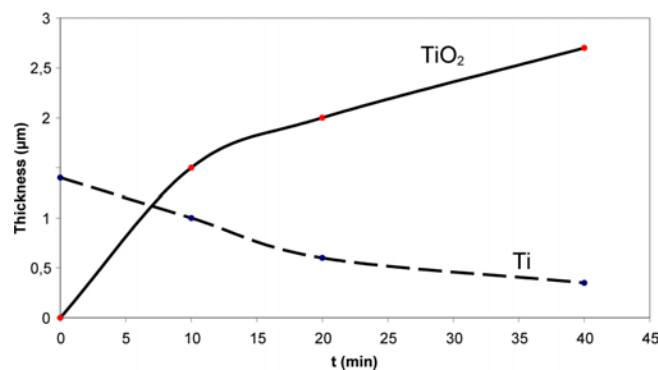
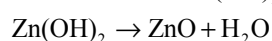
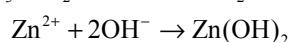
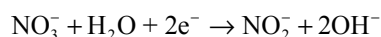


Figure 4 Thicknesses of Ti remaining layer and of TiO_2 nanotube film vs. anodisation time (see online version for colours)



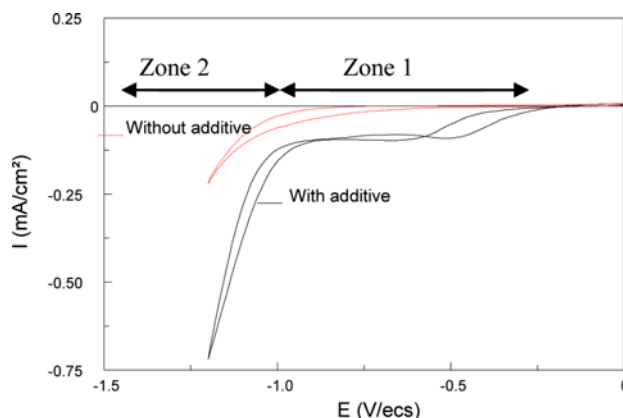
3.2 ZnO deposition on Ti foil

The electrochemical formation mechanism of ZnO is known to be initiated by the reduction of nitrate ions that produced hydroxide, followed by the precipitation of Zn(OH)₂. The conversion of Zn(OH)₂ into ZnO occurs in an ultimate step owing to the temperature effect [30,34]. The sequence of the ZnO deposition can be summarised by the following equations:



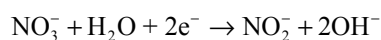
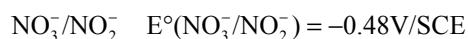
To highlight the deposition mechanism involved, voltammograms were performed on Ti electrode from zinc nitrate containing solution with and without additive (Figure 5). The reduction processes obtained are very different. In the additive-free electrolyte, a single increase in current occurs for a cathodic potential lower than -1 V (zone 2 in Figure 5). In the presence of additive, there are two reduction potential zones: the first (zone 1) shows an increase in current followed by a current plateau between -0.8 V and -1 V that indicates a diffusion control process. The second (zone 2) corresponds to that obtained without additive.

Figure 5 Voltammograms on Ti foil from zinc nitrate (0.005 M) + 0.005 M HMT electrolyte at 70°C (see online version for colours)



Three redox reactions can be considered:

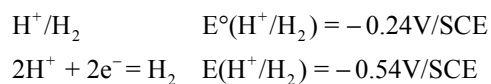
1 Redox couple



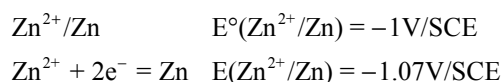
by neglecting NO₂⁻ concentration, we can calculate the equilibrium potential according to Nernst equation:

$$E(\text{NO}_3^- / \text{NO}_2^-) = -0.48 + 0.03 \text{Log}[\text{NO}_3^-] - 0.06 \text{Log}[\text{OH}^-] = 0.03\text{V/SCE}$$

2 Redox couple



3 Redox couple

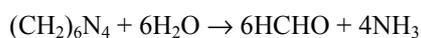


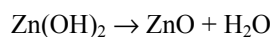
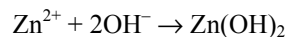
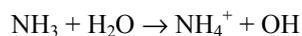
The examination of the potential values reveals that only the reduction of nitrate to nitrite ions can occur in zone 1 but this reaction is not favourable in an energetic point of view because of the reduction of anion on a cathodic electrode (negative surface). The two other reactions can take place only in zone 2.

Polarisations of Ti electrode were then performed at -0.9 V (zone 1) and -1.1 V (zone 2), during 3 min from both solutions. The SEM images obtained without additive are shown in Figure 6(A) and (B), whereas Figure 6(C) and (D) are obtained from additive-containing solution. In accordance with the voltammetric study, no deposit can be observed in Figure 6(A) confirming that the reduction of nitrate ions and then the precipitation of ZnO can only arise at a more cathodic applied potential. Actually, in Figure 6(B) spherical grains with a quite homogeneous size of about 300 nm in diameter appear at -1.1 V. The Energy Dispersive X-Ray Spectrum given in Figure 7 shows the presence of Ti, Zn and O elements. When HMT is added to the solution, some sticks lying on the Ti surface appear for a potential value of -0.9 V (Figure 6(C)). By increasing the cathodic applied potential (Figure 6(D)), a significant deposit is obtained while the shape of the grains is remained unchanged.

XRD analysis performed on deposits carried out at -1.1 V from both solutions is given in Figure 8. The experimental diffractograms were compared with the powder standard JCPDS (vertical line on the figure) of ZnO hexagonal würtzite phase (JCPDS File No: 00-036-1451) and the hexagonally closed packed structure of α -Ti (JCPDS File No: 44-1294) corresponding to the remaining Ti layer. In both cases, three peaks attributed to the ZnO structure are identified. Without additive (Figure 8(A)), no preferential orientation appears, the relative intensity of the peaks is in the same order than the values corresponding to the ZnO JCPDF files: $[101] > [100] > [002]$. From crystallites grown in the additive-containing solution, the $[002]$ intensity is slightly higher than the $[101]$ showing a preferential orientation in the c axis direction.

Combining the SEM and XRD analysis carried out on the bulk deposits with the voltammograms obtained in Figure 5, we assume that the current obtained in zone 2 is related to nitrate ions and proton reduction responsible for the ZnO formation. No metallic Zn deposit owing to the Zn^{2+} reduction could be obtained in this part of the curve, which is not in agreement with results reported in reference [36]. From additive-containing solution, the current plateau obtained in zone 1 can be related to the reduction of nitrate ions, which is enhanced by the presence of the additive. Otherwise, HMT is also added to chemical bath as precursor at high temperature (higher than 80°C during several hours) [35,47]. In this case, the chemical decomposition of HMT into ammonia can also lead to the formation of ZnO crystals according to the following reactions [48]:





However, the decomposition of HMT cannot be responsible for the current recorded on the voltammogram (only chemical reactions are involved), nor to the deposit obtained at -0.9 V in Figure 6(C) (temperature and duration are not sufficiently high). The accelerating effect owing to the HMT observed from both voltammetric study and SEM images can be related to an ion pairing mechanism, which has been already described by Franklin et al. [49]. This kind of ion pairing effect occurring for quaternary ammonium salts is expected to lower the energy barrier for adsorption of negatively charged species (NO_3^- in our case) onto the surface of the cathode.

Figure 6 SEM surface images obtained after the polarisation of Ti electrode during 3 min, from a 0.005 M zinc nitrate solution without additive (A) and (B) and with 0.005 M HMT (C) and (D) at different potentials

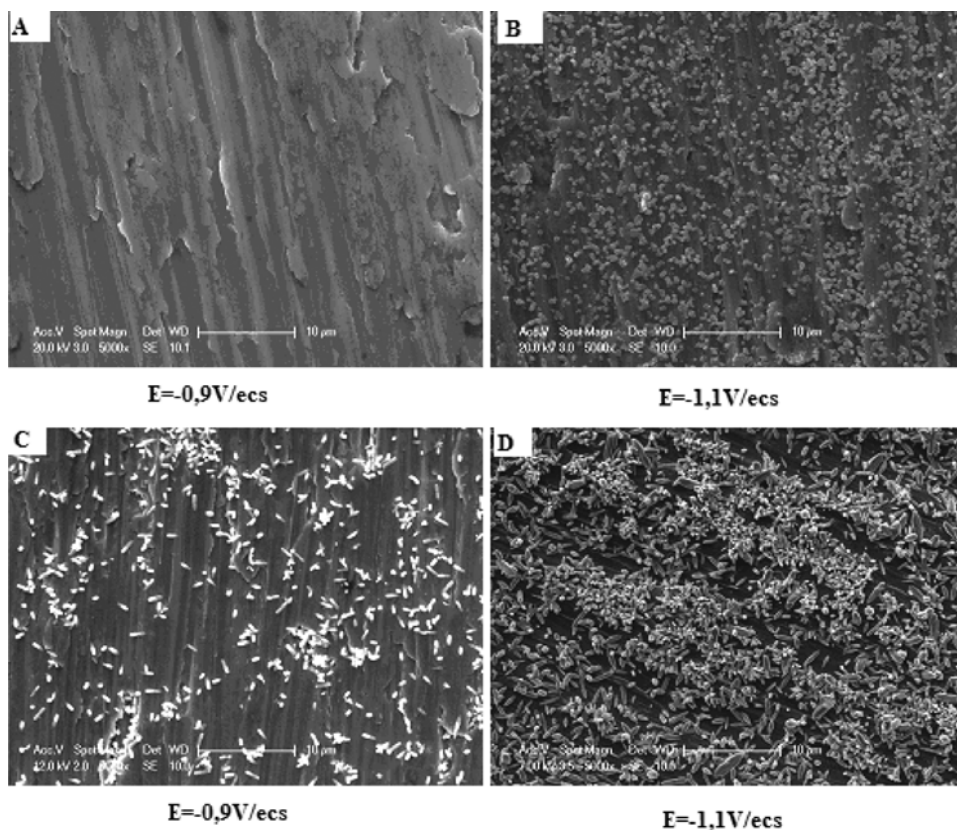


Figure 7 EDX analysis made on the surface shown in Figure 6(B) (see online version for colours)

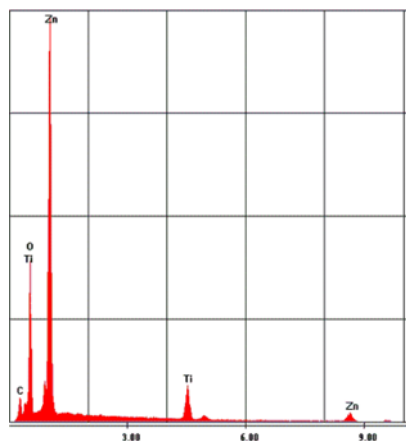
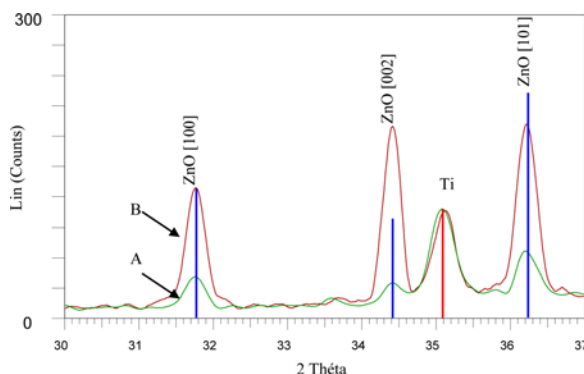


Figure 8 XRD patterns of ZnO rod arrays formed at -1.1 V from 0.005 M zinc nitrate electrolyte, at 70°C without additive (A), with 0.005M HMT (B) (see online version for colours)



3.3 ZnO deposition on TiO_2 nanotube arrays

The effect of the TiO_2 nanotube arrays on the ZnO deposition mechanism was firstly checked by voltammetry in a 0.005 M zinc nitrate solution (Figure 9). We can note that on TiO_2 , the reduction of nitrate ions gives rise to larger cathodic currents. In addition, the onset potential reaction on TiO_2 is found at -0.7 V, which is a lower cathodic potential than that obtained for Ti. This result demonstrates that the reduction reaction of nitrate ions on TiO_2 is thermodynamically enhanced. As a consequence, the precipitation of ZnO is enhanced too. The beneficial effect of TiO_2 may be due to the nature of the substrate as the strong increase in the surface owing to nanostructuring.

ZnO grains were deposited directly on both Ti thin film and titania nanotubes described in Figure 2(B). Potentiostatic experiments were carried out at 70°C in aqueous solution 0.005 M $\text{Zn}(\text{NO}_3)_2$, by applying -1.1 V/SCE during 10 min (Figure 10). Clearly, the morphology of ZnO is strongly influenced by the nature of the substrate. The

presence of the nanotubes leads to vertically oriented and densely packed grains showing a wire shape with an average diameter size of 250 nm (Figure 10(C) and (D)). For comparison, ZnO grains exhibit a globular structure without any orientation and an average size of 500 nm when deposition on performed on Ti substrate (Figure 10(A) and (B)).

Figure 9 Voltammograms from zinc nitrate (0.005M) electrolyte at 70°C on Ti substrate and on TiO₂ nanotube arrays

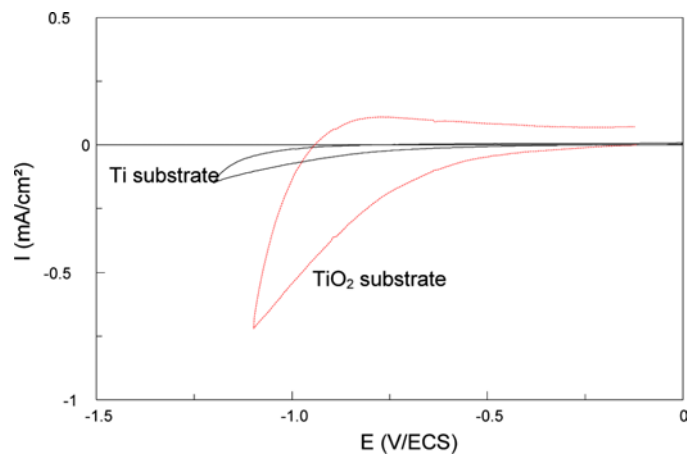
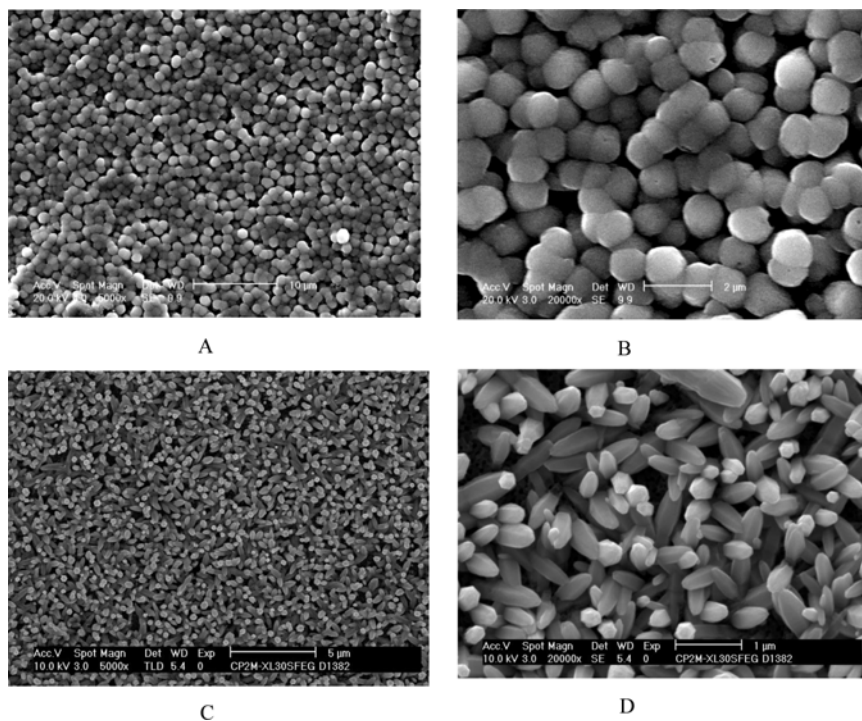
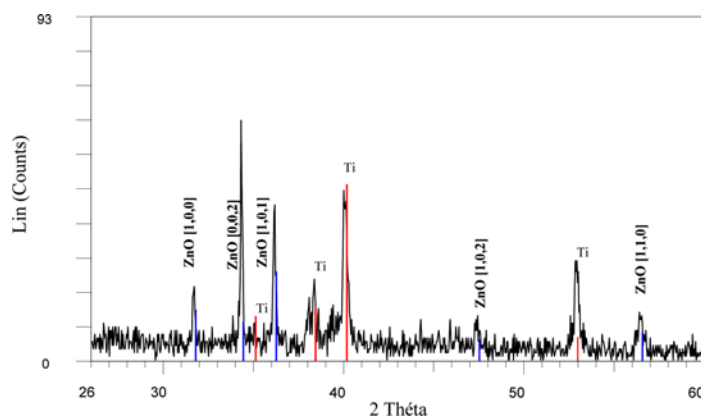


Figure 10 SEM images of ZnO layer deposited during 10 min on Ti thin film (A, B) and on titania nanotubes (C, D)



In Figure 11, it is represented the diffractogram established for ZnO deposit on TiO₂ nanotubes. The experimental diffractogram was also compared with the powder standard JCPDS (vertical line on the figure) of ZnO hexagonal phase and Ti corresponding to the remaining Ti layer. It can be noted that titania nanotubes are amorphous and therefore not present. Examination of XRD diagram confirms the formation of crystalline ZnO as well as the fact that growth occurs according to a preferred orientation. The sample indicates the presence of a (002) preferential orientation that differs from the (101) intense peak of the ZnO powder spectrum. The ZnO surface structuration obtained on TiO₂ nanotubes is significantly higher than that obtained from the additive-containing bath on Ti substrate. As it has been found in the previous work [44], the presence of nanotubes can modify the morphology of the electrodeposited layer and enhance the formation of vertical grains owing to a preferred orientation growth mechanism.

Figure 11 X-ray diffraction pattern performed on ZnO deposit on TiO₂ nanotubes corresponding to sample in Figure 10(C), showing the hexagonal ZnO phase and the preferred orientation of ZnO grains (see online version for colours)



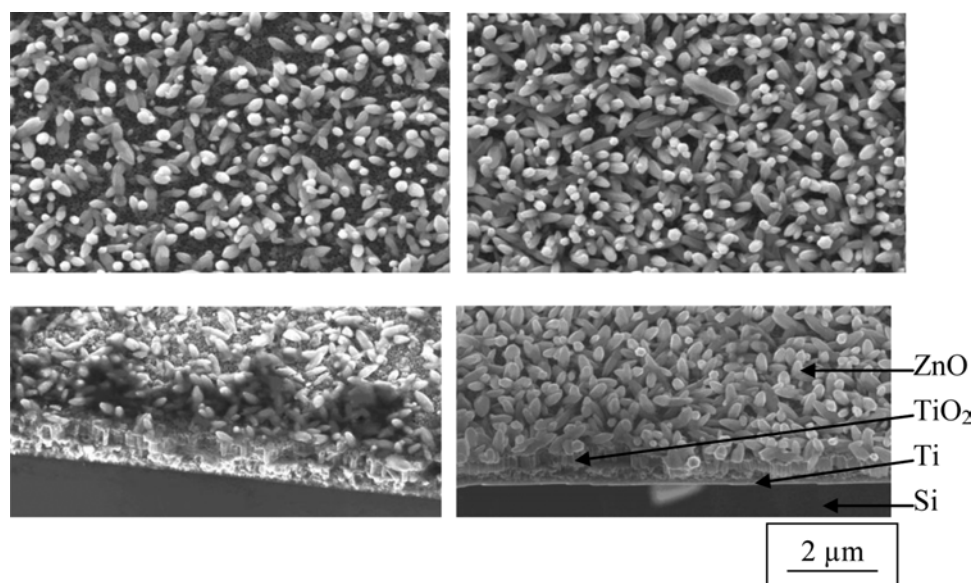
The influence of deposition time on the ZnO structure has also been studied. Figure 12(A) and (B) shows SEM images of ZnO grains grown onto nanotubes for 5 and 15 min. The corresponding cross-sectional images tilted at 30° are given in Figure 12(C) and (D). Clearly, the length of the ZnO grains increases with the deposition time while the diameter size is not modified (around 250 nm). The length of the particles is ranging from 500 nm to 800 nm after 5 min of deposition and from 1.2 μm to 1.9 μm after 15 min. It can be noted that the number of grains increases with increasing deposition time suggesting that a progressive growth mechanism is involved if nucleation occurs at the top surface of the nanotubes.

4 Conclusions

The electrochemical formation of ZnO crystallites has been studied using voltammetry. The effect of HMT was determined and the growth potential condition was optimised to obtain ZnO-oriented structure on Ti foil. ZnO rods have been also electrochemically deposited onto TiO₂ nanotubes grown from anodisation of Ti thin films. Besides the fact that titania nanotubes can be fabricated from a Ti thin film in a glycerol-containing

electrolyte, we demonstrated that the presence of the nanotubes can promote the wire-like shape of the ZnO grains. The simple procedure described in this work to achieve the fabrication of hybrid ZnO rods/titania nanotubes can be of potential interest for sensors, photovoltaics or photoelectrocatalytic applications.

Figure 12 ZnO deposited on titania nanotubes by applying -1.1 V/SCE during 5 min (A) and 15 min (B). The corresponding cross sections are shown in (C) and (D), respectively



References

- 1 Diebold, U. (2003) 'The surface science of titanium dioxide', *Surf. Sci. Rep.*, Vol. 48, pp.53–229.
- 2 Shankar, K.S. and Raychaudhuri, A.K. (2005) 'Fabrication of nanowires of multicomponent oxides: Review of recent advances', *Mater. Sci. Eng., C-Biomimetics Supramolecular Syst.*, Vol. 25, Nos. 5–8, pp.738–751.
- 3 Armstrong, A.R., Armstrong, G., Canales, J. and Bruce, P.G. (2005) 'TiO₂-B nanowires as negative electrodes for rechargeable lithium batteries', *J. Power Sources*, Vol. 146, Nos. 1–2, pp.501–506.
- 4 Berger, S., Macak, J.M., Kunze, J. and Schmuki, P. (2008) 'High-efficiency conversion of sputtered Ti thin films into TiO₂ nanotubular layers', *Electrochem. Solid-State Lett.*, Vol. 11, No. 7, pp.C37–C40.
- 5 Francioso, L., Taurino, A.M., Forleo, A. and Siciliano, P. (2008) 'TiO₂ nanowires array fabrication and gas sensing properties', *Sens. Actuators, B*, Vol. 130, No. 1, pp.70–76.
- 6 Jitputti, J., Suzuki, Y. and Yoshikawa, S. (2008) 'Synthesis of TiO₂ nanowires and their photocatalytic activity for hydrogen evolution', *Catal. Commun.*, Vol. 9, No. 6, pp.1265–1271.
- 7 Kitano, M., Matsuoka, M., Ueshima, M. and Anpo, M. (2007) 'Recent developments in titanium oxide-based photocatalysts', *Appl. Catal., A*, Vol. 325, No. 1, pp.1–14
- 8 Shiraiishi, Y. and Hirai, T. (2008) 'Selective organic transformations on titanium oxide-based photocatalysts', *J. Photochem. Photobiol., C*, Vol. 9, No. 4, pp.157–170.

- 9 Su, P.G., Sun, Y.L. and Lin, C.C. (2006) 'Novel low humidity sensor made of TiO₂ nanowires/poly(2-acrylamido-2-methylpropane sulfonate) composite material film combined with quartz crystal microbalance', *Talanta*, Vol. 69, No. 4, pp.946–951.
- 10 Jiang, Y.H., Wu, M., Wu, X.J., Sun, Y.M. and Yin, H.B. (2009) 'Low-temperature hydrothermal synthesis of flower-like ZnO microstructure and nanorod array on nanoporous TiO₂ film', *Mater. Lett.*, Vol. 63, No. 2, pp.275–278.
- 11 Wang, N., Li, X.Y., Wang, Y.X., Hou, Y., Zou, X.J. and Chen, G.H. (2008) 'Synthesis of ZnO/TiO₂ nanotube composite film by a two-step route', *Mater. Lett.*, Vol. 62, Nos. 21–22, pp.3691–3693.
- 12 Bestetti, M., Franz, S., Cuzzolin, M., Arosio, P. and Cavallotti, P.L. (2007) 'Structure of nanotubular titanium oxide templates prepared by electrochemical anodization in H₂SO₄/HF solutions', *Thin Solid Films*, Vol. 515, No. 13, pp.5253–5258.
- 13 Chen, X., Schriver, M., Suen, T. and Mao, S.S. (2007) 'Fabrication of 10 nm diameter TiO₂ nanotube arrays by titanium anodization', *Thin Solid Films*, Vol. 515, No. 24, pp.8511–8514.
- 14 Choi, J.S., Wehrspohn, R.B., Lee, J. and Gosele, U. (2004) 'Anodization of nanoimprinted titanium: a comparison with formation of porous alumina', *Electrochim. Acta*, Vol. 49, No. 16, pp.2645–2652.
- 15 Tang, Y.X., Tao, J., Zhang, Y.Y., Wu, T., Tao, H.J. and Zhu, Y.R. (2009) 'Preparation of TiO₂ nanotube on glass by anodization of Ti films at room temperature', *Trans. Nonferrous Met. Soc. China*, Vol. 19, No. 1, pp.192–198.
- 16 Yu, X.F., Li, Y.X., Wlodarski, W., Kandasamy, S. and Kalantar-Zadeh, K. (2008) 'Fabrication of nanostructured TiO₂ by anodization: A comparison between electrolytes and substrates', *Sens. Actuators, B*, Vol. 130, No. 1, pp.25–31.
- 17 Gong, D., Grimes, C.A., Varghese, O.K., Hu, W.C., Singh, R.S., Chen, Z. and Dickey, E.C. (2001) 'Titanium oxide nanotube arrays prepared by anodic oxidation', *J. Mater. Res.*, Vol. 16, No. 12, pp.3331–3334.
- 18 Zwillig, V., Aucouturier, M. and Darque-Ceretti, E. (1999) 'Anodic oxidation of titanium and TA6V alloy in chromic media. An electrochemical approach', *Electrochim. Acta*, Vol. 45, No. 6, pp.921–929.
- 19 Yasuda, K., Macak, J.M., Berger, S., Ghicov, A. and Schmuki, P. (2007) 'Mechanistic aspects of the self-organization process for oxide nanotube formation on valve metals', *J. Electrochem. Soc.*, Vol. 154, No. 9, pp.C472–C478.
- 20 Macak, J.M. and Schmuki, P. (2006) 'Anodic growth of self-organized anodic TiO₂ nanotubes in viscous electrolytes', *Electrochim. Acta*, Vol. 52, No. 3, pp.1258–1264.
- 21 LeClere, D.J., Velota, A., Skeldon, P., Thompson, G.E., Berger, S., Kunze, J., Schmuki, P., Habazaki, H. and Nagata, S. (2008) 'Tracer investigation of pore formation in anodic titania', *J. Electrochem. Soc.*, Vol. 155, No. 9, pp.C487–C494.
- 22 Ge, M.Y., Wu, H.P., Niu, L., Liu, J.F., Chen, S.Y., Shen, P.Y., Zeng, Y.W., Wang, Y.W., Zhang, G.Q. and Jiang, J.Z. (2007) 'Nanostructured ZnO: from monodisperse nanoparticles to nanorods', *J. Cryst. Growth*, Vol. 305, No. 1, pp.162–166.
- 23 Kao, P.C., Chu, S.Y., Li, B.J., Chang, J.W., Huang, H.H., Fang, Y.C. and Chang, R.C. (2009) 'Low temperature solution-synthesis and photoluminescence properties of ZnO nanowires', *J. Alloys Compd.*, Vol. 467, Nos. 1–2, pp.342–346.
- 24 Wang, M. and Zhang, L.D. (2009) 'The influence of orientation on the photoluminescence behavior of ZnO thin films obtained by chemical solution deposition', *Mater. Lett.*, Vol. 63, No. 2, pp.301–303.
- 25 Wu, G.S., Xie, T., Yuan, X.Y., Li, Y., Yang, L., Xiao, Y.H. and Zhang, L.D. (2005) 'Controlled synthesis of ZnO nanowires or nanotubes via sol-gel template process', *Solid State Commun.*, Vol. 134, No. 7, pp.485–489.
- 26 Zheng, M.J., Zhang, L.D., Li, G.H. and Shen, W.Z. (2002) 'Fabrication and optical properties of large-scale uniform zinc oxide nanowire arrays by one-step electrochemical deposition technique', *Chem. Phys. Lett.*, Vol. 363, Nos. 1–2, pp.123–128.

- 27 Wang, Y., Sun, Y. and Li, K. (2009) 'Dye-sensitized solar cells based on oriented ZnO nanowire-covered TiO₂ nanoparticle composite film electrodes', *Mater. Lett.*, Vol. 63, No. 12, pp.1102–1104.
- 28 Vayssieres, L. (2003) 'Growth of arrayed nanorods and nanowires of ZnO from aqueous solutions', *Adv. Mater.*, Vol. 15, No. 5, pp.464–466.
- 29 Chen, Z.G., Tang, Y.W., Zhang, L.S. and Luo, L.J. (2006) 'Electrodeposited nanoporous ZnO films exhibiting enhanced performance in dye-sensitized solar cells', *Electrochim. Acta*, Vol. 51, No. 26, pp.5870–5875.
- 30 Izaki, M. and Omi, T. (1996) 'Transparent zinc oxide films prepared by electrochemical reaction', *Appl. Phys. Lett.*, Vol. 68, No. 17, pp.2439–2440.
- 31 Pauporte, T. and Lincot, D. (1999) 'Heteroepitaxial electrodeposition of zinc oxide films on gallium nitride', *Appl. Phys. Lett.*, Vol. 75, No. 24, pp.3817–3819.
- 32 Peulon, S. and Lincot, D. (1998) 'Mechanistic study of cathodic electrodeposition of zinc oxide and zinc hydroxychloride films from oxygenated aqueous zinc chloride solutions', *J. Electrochem. Soc.*, Vol. 145, No. 3, pp.864–874.
- 33 Ramirez, D., Pauporte, T., Gomez, H. and Lincot, D. (2008) 'Electrochemical growth of ZnO nanowires inside nanoporous alumina templates. A comparison with metallic Zn nanowires growth', *Phys. Status Solidi A – Appl. Mater. Sci.*, Vol. 205, No. 10, pp.2371–2375.
- 34 Enculescu, I., Sima, M., Enculescu, M., Enache, M., Vasile, V. and Neumann, R. (2007) 'Influence of geometrical properties on light emission of ZnO nanowires', *Opt. Mater.*, Vol. 30, No. 1, pp.72–75.
- 35 Xu, F., Lu, Y.N., Xie, Y. and Liu, Y.F. (2009) 'Controllable morphology evolution of electrodeposited ZnO nano/micro-scale structures in aqueous solution', *Mater. Des.*, Vol. 30, No. 5, pp.1704–1711.
- 36 Wellings, J.S., Chaure, N.B., Heavens, S.N. and Dhannadasa, I.M. (2008) 'Growth and characterisation of electrodeposited ZnO thin films', *Thin Solid Films*, Vol. 516, No. 12, pp.3893–3898.
- 37 Stergiopoulos, T., Ghicov, A., Likodimos, V., Tsoukleris, D.S., Kunze, J., Schmuki, P. and Falaras, P. (2008) 'Dye-sensitized solar cells based on thick highly ordered TiO₂ nanotubes produced by controlled anodic oxidation in non-aqueous electrolytic media', *Nanotechnology*, Vol. 19, No. 23, pp.235602.
- 38 Baxter, J.B. and Aydil, E.S. (2006) 'Dye-sensitized solar cells based on semiconductor morphologies with ZnO nanowires', *Sol. Energy Mater. Sol. Cells*, Vol. 90, No. 5, pp.607–622.
- 39 Lee, W., Kang, S.H., Kim, J.Y., Kolekar, G.B., Sung, Y.E. and Han, S.H. (2009) 'TiO₂ nanotubes with a ZnO thin energy barrier for improved current efficiency of CdSe quantum-dot-sensitized solar cells', *Nanotechnology*, Vol. 20, No. 33, pp.335706–335712.
- 40 Zhang, Z.H., Yuan, Y., Liang, L.H., Cheng, Y.X., Shi, G.Y. and Jin, L.T. (2008) 'Preparation and photoelectrocatalytic activity of ZnO nanorods embedded in highly ordered TiO₂ nanotube arrays electrode for azo dye degradation', *J. Hazard. Mater.*, Vol. 158, Nos. 2–3, pp.517–522.
- 41 Ortiz, G.F., Hanzu, I., Lavela, P., Tirado, J.L., Knauth, P. and Djenizian, T. (2010) 'A novel architected negative electrode based on titania nanotube and iron oxide nanowire composites for Li-ion microbatteries', *J. Mater. Chem.*, Vol. 20, No. 20, pp.4041–4046.
- 42 Ortiz, G.F., Hanzu, I., Lavela, P., Knauth, P., Tirado, J.L. and Djenizian, T. (2010) 'Nanoarchitected TiO₂/SnO: a future negative electrode for high power density li-ion microbatteries?', *Chem. Mater.*, Vol. 22, No. 5, pp.1926–1932.
- 43 Ortiz, G.F., Hanzu, I., Knauth, P., Lavela, P., Tirado, J.L. and Djenizian, T. (2009) 'Nanocomposite electrode for Li-Ion microbatteries based on SnO on nanotubular titania matrix', *Electrochem. Solid-State Lett.*, Vol. 12, No. 9, pp.A186–A189.

- 44 Hanzu, I., Djenizian, T., Ortiz, G.F. and Knauth, P. (2009) 'Mechanistic study of Sn electrodeposition on TiO₂ nanotube layers: thermodynamics, kinetics, nucleation, and growth modes', *J. Phys. Chem. C*, Vol. 113, No. 48, pp.20568–20575.
- 45 Djenizian, T., Hanzu, I., Eyraud, M. and Santinacci, L. (2008) 'Electrochemical fabrication of tin nanowires: a short review', *C.R. Chim.*, Vol. 11, No. 9, pp.995–1003.
- 46 Premchand, Y.D., Djenizian, T., Vacandio, F. and Knauth, P. (2006) 'Fabrication of self-organized TiO₂ nanotubes from columnar titanium thin films sputtered on semiconductor surfaces', *Electrochem. Commun.*, Vol. 8, No. 12, pp.1840–1844.
- 47 Yang, M., Yin, G.F., Huang, Z.B., Liao, X.M., Kang, Y.Q. and Yao, Y.D. (2008) 'Well-aligned ZnO rod arrays grown on glass substrate from aqueous solution', *Appl. Surf. Sci.*, Vol. 254, No. 10, pp.2917–2921.
- 48 Vernardou, D., Kenanakis, G., Couris, S., Manikas, A.C., Voyiatzis, G.A., Pemble, M.E., Koudoumas, E. and Katsarakis, N. (2007) 'The effect of growth time on the morphology of ZnO structures deposited on Si (100) by the aqueous chemical growth technique', *J. Cryst. Growth*, Vol. 308, No. 1, pp.105–109.
- 49 Franklin, T.C., Totten, V. and Aktan, A. (1988) 'Ion-pairing as a mechanism of action of additives in electrodeposition', *J. Electrochem. Soc.*, Vol. 135, No. 7, pp.1638–1640.